Schottky barriers on phosphorus-doped hydrogenated amorphous silicon: The effects of tunneling

W. B. Jackson, R. J. Nemanich, M. J. Thompson, and B. Wacker
Xerox Corporation, Palo Alto Research Center, Palo Alto, California 94304
(Received 5 December 1985)

A systematic investigation of the transport properties of PtSi on phosphorus-doped hydrogenated amorphous silicon (*a*-Si:H) interfaces is presented. The transition from rectifying Schottky barriers to Ohmic contacts is observed as the doping level is increased. The barrier heights of PtSi on *a*-Si:H versus doping concentration and applied bias are measured with use of internal photoemission. In addition, the activation energy, ideality factor, flat-band voltage, and reverse-bias current-voltage characteristics are also determined. The results are analyzed in terms of the theory for thermionic-field-emission tunneling through the barrier. The agreement indicates that tunneling is extremely important for barriers on all but the lowest-doped *a*-Si:H at room temperature. While a change ~ 0.6 eV of the effective barrier height is observed, the analysis indicates that the actual barrier height is independent of doping despite a change in the Fermi level of ~ 0.4 eV. No evidence for the lowering of the barrier due to phosphorus-induced donor levels is found. The origin of the barrier formation and evolution of the electrical characteristics of the contact as a function of doping are discussed.

I. INTRODUCTION

The band discontinuity at a metal-semiconductor interface, or the Schottky barrier, is due to the alignment of the bulk electronic levels or to interface states which lie energetically within the semiconductor band gap. The details of the origin of the Schottky barrier for even well-studied metals on crystalline Si (*c*-Si) is still not well understood because interface densities as low as $\sim 10^{13}$ cm^{-2} can pin the Fermi energy at the interface. Since the interface properties often dominate the bulk electrical response of the semiconductor, the understanding of the electrical properties of this metal-semiconductor interfacial barrier is critical for a complete interpretation of most electrical measurements.

It has been shown that the interface of metals and hydrogenated amorphous silicon (*a*-Si:H), as in the case of *c*-Si, often results in a contact with rectifying behavior.[1] The characteristics of the interface are in some ways similar to the Schottky barrier of crystalline Si, but the unique electronic properties of amorphous semiconductors such as localized states near the band edge, make the problem quite different from crystalline semiconductors. In this study, the electrical characteristics of Pt/*a*-Si:H interfaces are probed as a function of doping of the *a*-Si:H. The goal is to examine the barrier properties as the depletion region becomes smaller and as the Fermi energy moves from midgap to near the *a*-Si:H conduction band. Pt/*a*-Si:H structures were chosen because the solid-state reactions leading to PtSi formation have been well studied[2] and because a high barrier is obtained.

For crystalline silicon there is a relatively good understanding of the conditions which can lead to a metal-semiconductor interface exhibiting Ohmic or rectifying behavior. Consider the schematic of the bands at a metal-semiconductor interface shown in Fig. 1. While the Schottky barrier is the band discontinuity between the metal and the semiconductor conduction band, the effective barrier is determined by the dominant current mechanism. In the case of light doping in the semiconductor, high temperatures, and/or moderate fields, the dominant current transport is due to thermal excitation above the barrier. This current is known as the thermionic-emission current.[3] The contribution of the current due to tunneling increases if (1) the doping of the semiconductor increases causing the depletion region to narrow, (2) the tempera-

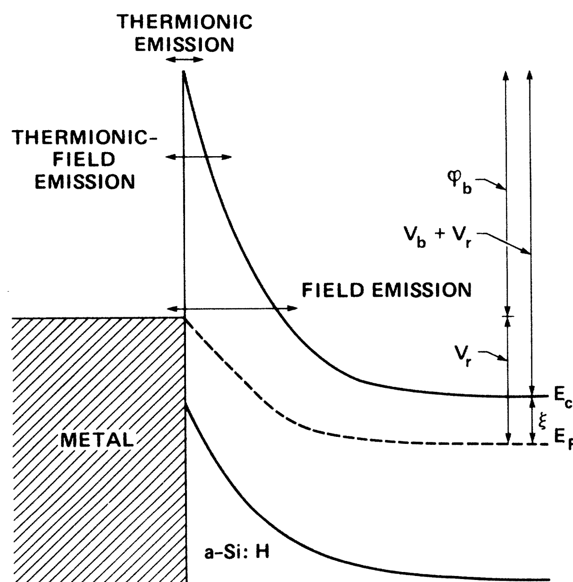

FIG. 1. Band diagram for a metal—*a*-Si:H Schottky barrier with definitions of symbols defined in the text. The various current paths for various tunneling regimes is also indicated.

©1986 The American Physical Society

ture is lowered sufficiently to eliminate the transport over the barrier, and/or (3) if the field is increased by a large reverse bias. In an intermediate regime, the dominant current may be described as thermally assisted tunneling and is known as the thermionic-field-emission current. Under conditions which result in a collapse of the depletion region, the dominant current transport occurs from the metal Fermi level to the semiconductor conduction band and becomes a field-emission current. Such a contact is no longer rectifying and is Ohmic since the current is more or less proportional to the applied voltage irrespective of polarity.

This continuous transformation between the rectifying and Ohmic contacts is reasonably well explained in *c*-Si by the theory of thermionic-field emission which calculates the tunneling current through a parabolic barrier using the WKB approximation.[4,5] This theory also accounts for the lowering of the effective barrier upon increasing reverse bias and/or doping.

Despite considerable efforts aimed at understanding certain aspects of the electrical properties of *a*-Si:H Schottky barriers and the solid-state reactions at the metal—*a*-Si:H interface, the evolution of the electrical characteristics from blocking to Ohmic contacts is not well understood. Current-voltage (I-V),[6–8] capacitance-voltage (C-V),[6,9,10] and internal photoemission[6,11–14] measurements have been used to characterize the barrier, while time-of-flight measurements have been used to probe the depletion region.[15] Although most efforts have concentrated on undoped *a*-Si:H, several investigations of Schottky barriers on doped *a*-Si:H have found that the barrier height apparently decreases as the phosphorus doping increases[6,16,17] and that the ideality factor increases with decreasing temperature.[17] One investigation of Schottky barriers on heavily doped *a*-Si:H, has suggested that the thermionic-field-emission theory for *c*-Si may explain the breakdown characteristics of the rectifying contact at large reverse biases.[9]

The observed barrier lowering with increasing doping has been accounted for with several models. Two groups have attributed this effect to the creation of a specific donor-level conduction path located $\sim$0.3 eV below the conduction-band mobility edge.[6,17] The phosphorus donor level was suggested to give rise to an alternate conduction path lowering the effective barrier. It has also been suggested that the electronic properties of the doped *a*-Si:H have resulted in a change in the Schottky-barrier height. A final possibility is that the collapse of the depletion region will cause a lowering of the effective barrier, but since the barrier properties of amorphous and crystalline Si are different, the analysis must be modified.

While the proposal of tunneling to states attributed to the phosphorus donor band may seem correct, there have been several recent measurements which contradict this possibility. First, from hyperfine measurements[18] and from the activation energy of the conductivity for heavily P-doped samples, the phosphorus donor band is known to be less than 0.18 eV below the conduction band, a value the Fermi level will not exceed. In the absence of tunneling, the P donor level cannot result in a barrier lowering of 0.3—0.4 eV since the P donor level is less than 0.18 eV below the conduction-band edge. The hyperfine measurements also indicate that the donor-level density of states exceeds the tail-state density only for doping levels above 10^{-4} in the gas phase, while there is significant lowering for doping as low as 1×10^{-5}. Finally, time-of-flight measurements have found little change in the electron mobility for low to moderate phosphorus doping levels.[19] This result demonstrates that the conduction-band tail states are not altered by a phosphorus donor band.

In the present work, the barrier heights are measured as a function of doping and bias dependence using internal photoemission. The Fermi level of the phosphorus-doped *a*-Si:H is measured to determine the built-in potential (or the band bending). The results are in quantitative agreement with the thermionic-field-emission model. The data show that the rectifying contact evolves into an Ohmic contact by increased tunneling and lowering of the effective barrier. There is no evidence for a lowering of the barrier due to a donor-level conduction path 0.3 eV below the mobility edge; the results can be explained without resort to a specific level below the mobility edge. Finally, the evolution of the barrier height and flat-band voltage as a function of doping is discussed in terms of current models for Schottky-barrier formation at the metal—*a*-Si:H interface.

II. THEORY

Tunneling and thermionic-field emission in *c*-Si have been investigated in a number of papers.[3–5] The approach used in most theories is to determine the tunneling through a barrier of an appropriate shape (usually a parabolic or truncated parabolic band to include the image-force lowering) using the WKB approximation. Since this approach quickly leads to nonanalytic expressions, some authors such as Padovani and Stratton[4] have approximated the energy distribution of the carriers emitted through the barriers by a Gaussian distribution with a peak which depends on the barrier thickness and temperature. Crowell and Rideout, on the other hand, have numerically evaluated the tunneling expressions.[5] In general, the analytic approximation[4] yields results which are in fair agreement with the more exact calculation although the expressions tend to underestimate the tails of the electron distribution and, hence, the effects of tunneling.[5] Because the analytic expressions reveal the functional dependence of the tunneling, we will compare our *a*-Si:H results with the theory of Padovani and Stratton to determine whether the functional-dependence of the theory and the data for *a*-Si:H are consistent. It is important to note that precise quantitative agreement for *a*-Si:H is not necessarily expected since, even for *c*-Si, the theory is approximate, yielding only semiquantitative agreement with experiment. The agreement found for *a*-Si:H between the theory and experiment is remarkably close considering, particularly, our lack of precise knowledge of some important parameters of the contacts to *a*-Si:H, such as the doping efficiency and the effective tunneling mass.

Throughout our analysis we will assume that the limiting mechanism of transport through the depletion region and into the metal will be the thermionic emission and not

the diffusion of carriers. These two processes can be viewed as acting in series; therefore, the current transport will in general be dominated by one effect. For well-formed and characterized PtSi/a-Si:H structures, the temperature dependence of the I-V characteristics have been shown to be consistent with thermionic emission.[13]

According to the theory presented in Ref. 4, the reverse saturation current of a diode with tunneling contributions is given by

$$J = J_s \exp(V_r/E') , \tag{1}$$

where J_s is the reverse saturation current, V_r is the reverse bias voltage (defined as positive for a negative bias applied to the metal), and E' is given below. We note that in general, if tunneling is important, the reverse saturation current will exhibit an exponential dependence on voltage. In particular, E' is given by

$$E' = E_{00}/[qE_{00}/kT - \tanh(qE_{00}/kT)] , \tag{2}$$

where T is the temperature, k is Boltzmann's constant, q is the electron charge, and E_{00} (in eV) is given by

$$\begin{aligned} E_{00} &= \hbar(N_d/m_r\epsilon_s)^{1/2}/2 \\ &= 18.5\times10^{-12}(N_d/m_r\epsilon_s)^{1/2} , \end{aligned} \tag{3}$$

where N_d is the donor density in cm^{-3}; m_r is the effective mass in terms of m, the free-electron mass, and ϵ_s is the relative dielectric constant. E_{00} has the physical interpretation of being the height of a barrier where the tunneling probability is e^{-1} for electrons at the semiconductor band edge. Thus the parameter qE_{00}/kT is a rough measure of the relative importance of tunneling. If $qE_{00}/kT \ll 1$, thermal excitation over the barrier is dominant, while if $qE_{00}/kT \sim 1$ then the current is thermionic-field emission predominates. The current becomes a field-emission current when $qE_{00}/kT > 1$. A more precise delineation between the various regimes may be found in Ref. 5.

Because E_{00} is a fundamental quantity for the theory of tunneling, it is important to discuss the values of the parameters $\epsilon_s m_r$ and N_d used in determining its value for a-Si:H. In the case of c-Si, best agreement between theory and experiment is obtained if $\epsilon_s m_r$ is taken to be 2.5.[3] This value requires that m_r be 0.2, which is somewhat low and is probably due to the approximations used in the thermionic-field-emission theory. N_d is equal to the dopant density since nearly all dopants are fourfold coordinated in c-Si and, hence, electrically active.

In the case of a-Si:H, there is some uncertainty in relating the donor density to the gas-phase dopants because the dopants may be threefold coordinated. A threefold-coordinated phosphorus atom will be neutral and will not contribute to the space-charge layer that determines the barrier shape. Threefold-coordinated dopants will not affect the tunneling and one must therefore find a relation between the charged defect density and the gas-phase dopant concentration.

According to the "$8-N$" model for doping in a-Si:H,[20] a phosphorus atom is incorporated into a fourfold configuration only if a negatively charged dangling bond is created at the same time. Consequently, the number of donors and defects should be equal. The donor density N_d can be determined from the subgap defect density measured by photothermal deflection spectroscopy[21] and luminescence[20] and roughly follows the relation $N_d \simeq [\text{PH}_3]^{0.5}$. The uncertainties due to the actual dopant-incorporation measurement preclude a more precise determination of the donor density. With the above uncertainties in mind, we use defect values previously reported for doping-induced defect densities found by photothermal deletion in Table I.[21] We also treat $\epsilon_s m_r$ as a free parameter and fit the voltage dependence of the barrier height for the 1×10^{-6} sample. In this case, we get reasonable agreement for $\epsilon_s m_r \simeq 0.5$ if $N_d \sim [\text{PH}_3]^{0.5}$. Depending on the exact relation between the number of donors and the gas-phase concentration, the thermionic emission should dominate for doping as high as 10^{-4} in the gas phase. Using Eq. (3), we find that a room temperature, $qE_{00}/kT \sim 1$ for a doping density of 10^{-3} P. Tunneling is expected to dominate for these doping densities.

The reverse saturation current J_s is given by

$$J_s = J_{s0} \exp(-\varphi_b/E_0) , \tag{4}$$

where φ_b is the barrier height without tunneling (see Fig. 1), and

$$E_0 = E_{00} \coth(qE_{00}/kT) . \tag{5}$$

J_{s0} is weakly dependent on voltage and is given by

$$\begin{aligned} J_{s0} &= A^* T(\pi q E_{00})^{1/2} \\ &\quad \times [q(V_r - \xi) + q\varphi_b/\cosh^2(qE_{00}/kT)]^{1/2}/k . \end{aligned} \tag{6}$$

A^* is Richardson's constant and $q\xi$ is the energy from the Fermi level to the conduction band in the doped semiconductor.

TABLE I. Schottky-barrier parameters for various doping levels.

Doping	N_d (cm^{-3})	ξ (eV)	V_b (eV)	φ_{eff} (eV)	at V_r (V)	φ_b (eV)	φ_b^* (eV)
Undoped	3×10^{15}	0.82	0.34	1.16	2.00	1.16	1.14
2.5×10^{-7}	1.4×10^{16}	0.36	0.79	1.13	2.00	1.15	1.15
1.0×10^{-6}	2.2×10^{16}	0.25	0.87	1.10	1.50	1.12	1.15
1.0×10^{-5}	1.0×10^{17}	0.21	0.86	0.98	1.90	1.07	1.16
1.0×10^{-4}	2.5×10^{17}	0.15	0.73	0.70	1.50	0.88	1.12
1.0×10^{-3}	1.0×10^{18}	0.15	0.74	0.52	0.66	0.89	1.04

When $qE_{00}/kT \ll 1$, the thermionic-emission case, $E_0 = kT/q$ and Eq. (4) becomes $J = J_{s0}\exp(-q\varphi_b/kT)$, the standard diode expression for the reverse bias current. We may define an effective barrier height when tunneling is important by the relation

$$J = J_{s0}\exp(-q\varphi_{\text{eff}}/kT)$$
$$= J_{s0}\exp(-\varphi_b/E_0)\exp(V_r/E') , \quad (7)$$

or

$$\varphi_{\text{eff}} = (kT/q)(\varphi_b/E_0 - V_r/E') . \quad (8)$$

When tunneling predominates, Eq. (8) predicts that the barrier height decreases linearly with increasing reverse bias. The slope of the decrease for small reverse biases is

$$\frac{d\varphi_{\text{eff}}}{dV_r} = -kT/qE'$$
$$\simeq -(qE_{00}/kT)^2/3 \propto N_d \quad (qE_{00}/kT \ll 1) . \quad (9)$$

Thus the rate of barrier lowering due to increased applied bias increases with doping. For 10^{18} donors/cm^{-3}, the rate of barrier lowering for *a*-Si:H is roughly 0.05 eV/V, and the effective barrier disappears extremely rapidly for comparatively small reverse biases.

Not only does the barrier decrease with voltage, but the increased doping lowers the effective barrier at zero-bias barrier as well, according to the relation

$$\varphi_{\text{eff}}(V_r = 0) = kT\varphi_b[\tanh(qE_{00}/kT)]/qE_{00} . \quad (10)$$

For $qE_{00}/kT \ll 1$,

$$\varphi_{\text{eff}}(V_r = 0) \simeq [1 - (qE_{00}/kT)^2/3]\varphi_b , \quad (11)$$

demonstrating that the rate the zero-bias barrier-height decrease is proportional to the donor density. When $qE_{00}/kT > 1$,

$$J_s = J_{s0}\exp(-\varphi_b/E_{00}) . \quad (12)$$

The reverse saturation current no longer depends on temperature, or equivalently, the ideality factor is roughly inversely proportional to the temperature. For a donor density of 10^{19} cm^{-3}, $E_{00} \simeq 3kT$, the effective barrier is one-third of its low-doping value and decreases with reverse bias at a rate of ~ 1.0 eV/V. The barrier, in essence, no longer exists.

III. EXPERIMENTAL DETAILS

A. Samples

The samples used in this experiment consisted of the following structures. The substrates were crystalline Si overcoated with 100 nm of evaporated Cr and a 30-nm n^+ layer of 10^{-2} doped amorphous silicon which formed the Ohmic backcontact. The active layer of *a*-Si:H was 1.8 μm thick and was doped by the introduction of phosphine in the gas-phase concentrations relative to the silane ranging from 2.5×10^{-7} to 10^{-3} during deposition. The doped *a*-Si:H was deposited at low rf powers under conditions known to produce optimal material. The final layer consisted of 2-mm-diam electrodes of 8-nm-thick Pt. In order to ensure silicide formation, the samples were etched immediately prior to the Pt deposition and were annealed at 200 °C for 30 min in the Pt-deposition system. This procedure is known to cause a solid-state reaction and form the crystalline compound PtSi.[13] This procedure also eliminates the interfacial oxide layer.

B. Electrical measurements

A number of electrical measurements were performed on the samples. First, *I-V* measurements were made for both forward and reverse biases. The forward-bias current-versus-voltage curves were used to extract the ideality factor for the diodes.[7] The sample structures with the smallest ideality factors were used for all the other measurements. The ideality factor became significantly larger as the doping increases.

The spectral dependence of the photoconductivity was determined for various reverse biases. The illumination source consisted of a quartz tungsten lamp dispersed by a $\frac{1}{4}$-m monochromator with ~ 13-nm resolution. The exciting light was chopped at 7 Hz, while the synchronous photocurrent was detected using a current preamp and a lock-in amplifier. The incident photon flux was measured by a pyroelectric detector. The spectral dependence of the number of carriers collected per incident photon or photoconductive yield, *Y*, was determined.

The barrier heights were determined from the spectral dependence of the photoconductive yield using the theory of internal photoemission. According to this theory, the spectral dependence of the photoconductive yield due to transitions over the Schottky barrier (transition *A* in Fig. 2) is related to the barrier height by the equation

$$Y \sim (\hbar\omega - \varphi_b)^2 \quad \text{for } \hbar\omega > \varphi_b , \quad (13)$$

where $\hbar\omega$ is the photon energy. The barrier is determined from Eq. (13) by computing the zero intercept of $Y^{1/2}$ below the band gap versus photon energy. In order to determine the barrier height accurately, the yield due to

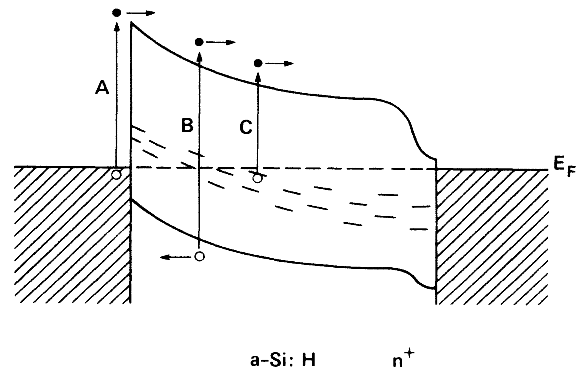

FIG. 2. Various transitions possible in a reverse-bias Schottky barrier under illumination. Transition *A* gives rise to internal photoemission, *B* is the band-to-band transition, *C* is a transition from a defect level to the conduction band, and *D* is the band-to-band transition in the Ohmic backcontact.

internal photoemission (transition A in Fig. 2) must be distinguished from that due to band-to-band excitations (transition B). This separation of the two contributions is aided by doping. Both the electrons and holes generated by the band-to-band transitions must be collected in order to contribute to the steady-state current (further discussion is given in Sec. IV). Since phosphorus doping decreases the hole lifetime significantly, the band-to-band collection efficiency is reduced. This results in an enhancement of the internal photoemission with respect to band-to-band transitions, because in the case of internal photoemission the holes are created in the metal layer.

The voltage dependence of the barrier height for a given sample was determined by measuring the spectral dependence of the reverse-bias yield as the bias voltage was increased. Relative changes in the barrier heights as small as 3 meV could be determined by keeping the sample position fixed, repeating the measurements at the same wavelengths, and fitting the data to Eq. (13) over the same energy range for each voltage. The sample-to-sample fluctuations in barrier heights are $\sim$0.07 eV due to slight variations in alignment and sample thicknesses. The ac photocurrent versus applied bias was determined by keeping the photon energy constant.

The energy separation between the conduction band and the Fermi level was determined for each doping by using capacitance and current methods. For the heavily-doped samples, the activation energy was determined by measuring the capacitance as a function of temperature for various measurement frequencies. The capacitance decreases to the geometrical capacitance at carrier freeze-out (Fig. 3). The slope of a line obtained by plotting the natural logarithm of the freeze-out frequency versus $1/kT$ yields the activation energy (inset, Fig. 3). The advantage of this method is that the effects of band bending on the bulk activation energy are eliminated. For the lightly doped samples (1×10^{-6} and 2.5×10^{-7} PH_3), freeze-out occurred above room temperature even for 10 Hz, requiring the use of another method. The activation energy of the far-forward-bias current at 3 V was measured for temperatures between 100 and 200 K for the lightly doped samples. The two methods yielded identical results for the 1×10^{-5} sample, demonstrating that the forward-bias measurement yields reliable results for the more lightly doped samples.

The built-in potential was also estimated by measuring the photocurrent at a fixed wavelength versus applied voltage. The forward-bias voltage at which the photocurrent changes sign is a rough indication of the built-in potential. However, this procedure is valid only if tunneling is not significant. Since tunneling will be shown below to be extremely important for medium to heavy doping levels, this method yields low values for the built-in potential.

IV. RESULTS

Consider first the reverse- and forward-bias I-V measurements. Saturation of the reverse current is expected if the current transport is solely by thermionic emission. The reverse-bias current for various doping levels is shown in Fig. 4. Saturation is not observed, and the current is more or less exponential with a slope that increases as the doping increases. The magnitude of the current becomes extremely large for higher doping. This result indicates that the rectification decreases as expected from previous measurements. The forward-bias currents were used to determined the ideality factors for various doping levels; the results are shown in Fig. 5. Also shown is the temperature dependence of the ideality parameter for the 1×10^{-5} doped sample. The ideality parameters are plotted versus the parameter, kT/E_{00}, which is proportional to $N_d^{-1/2}$. The experiments indicate that the

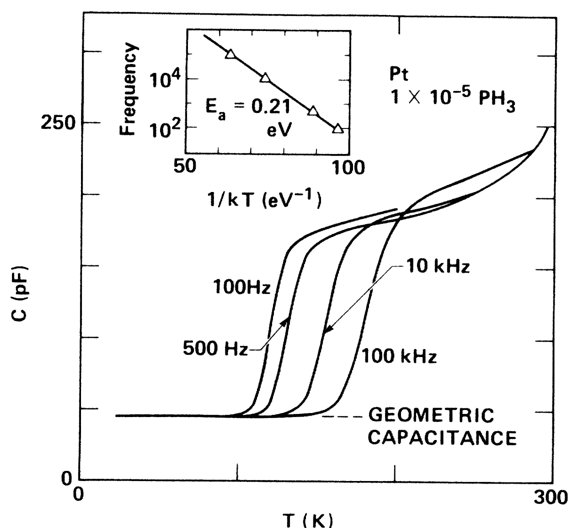

FIG. 3. Capacitance of a 1×10^{-5}-PH_3-doped sample versus temperature for various frequencies. The activation energy is determined from the slope of an Arrhenius plot of the inverse of the temperature of maximum slope (carrier freeze-out) versus the logarithm of the measuring frequency (inset).

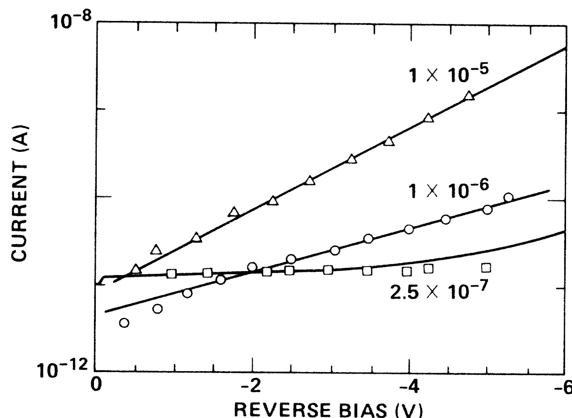

FIG. 4. The points indicate the reverse-bias current versus reverse bias for various doping levels. The solid lines are determined by substituting the measured voltage dependence of the barrier height from Fig. 9 into Eq. (7).

ideality parameter becomes larger for both increasing doping levels and lower temperatures.

The barrier height was determined by measuring the spectral dependence of the photoresponse. The photoconductive yield Y is plotted versus photon energy E for various doping levels in Fig. 6. The band-to-band transitions (transition B in Fig. 2) gives rise to the large yields for energies above 1.5 eV. Below 1.5 eV the yield is due to the internal photoemission (transition A in Fig. 2) and can be extrapolated to give the barrier height using Eq. (13). The carriers for the internal photoemission are generated in the thin metal layer, and will therefore be very sensitive to optical interference within the sample. The large interference fringes in the spectral region due to the internal photoemission are characteristic of this effect. The increase of the yield below 1.5 eV with increased doping is,

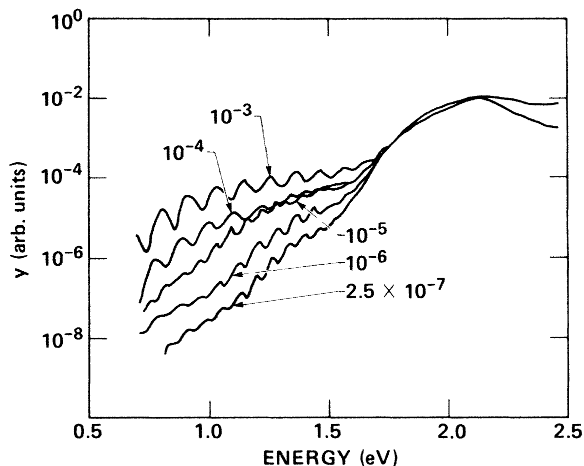

FIG. 6. Photoconductive yield versus photon energy for various doping levels. Curves are normalized at 2.1 eV. The oscillations are due to interference fringes.

in general, an indication of the lowering of the effective barrier height. Figure 7 and Table I show that the zero-bias barrier decreases as the doping increases.

An additional spectra feature appears in the photoresponse below 1 eV for the lower doping levels In this region the. fringes are reduced. The photocurrent is plotted versus time in Fig. 8. The photocurrent decays after the light is turned on, and exhibits the unusual effect of exhibiting a negative current after the illumination is turned off. This result can be explained by transitions from occupied defect levels to the conduction band (transition C in Fig. 2). Initially, light excites electrons from the deep centers to the conduction band where the electrons drift to the backcontact. The holes left behind are deeply trapped and are not collected. Consequently, the sample builds up a positive space charge which collapses the field during the light pulse, decreasing the collection of subsequent electrons and the photocurrent even though

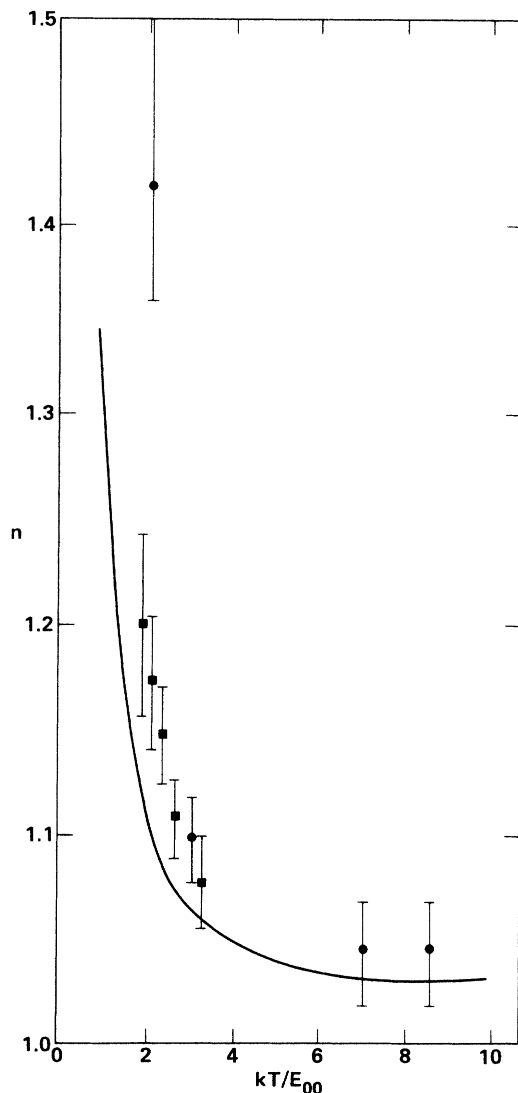

FIG. 5. The points indicate the measured ideality factor for various doping levels at room temperature (circles) and for a 10^{-5}-P-doped sample for different temperatures (squares). The solid line is the result of the theory showing the increase in ideality factor due to tunneling.

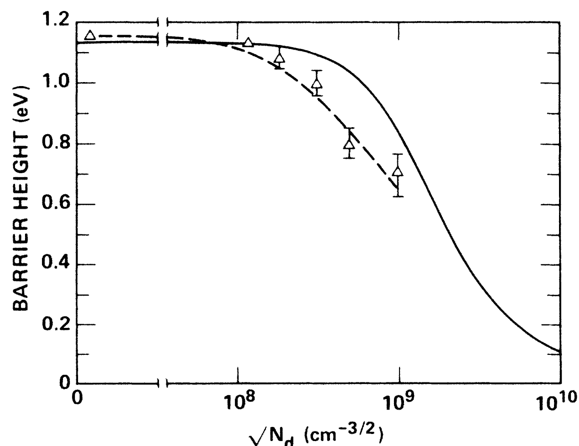

FIG. 7. The points indicate the barrier heights corrected for zero volts bias versus the square root of the donor density for each doping level. The solid line is the theoretical expression using Eq. (8).

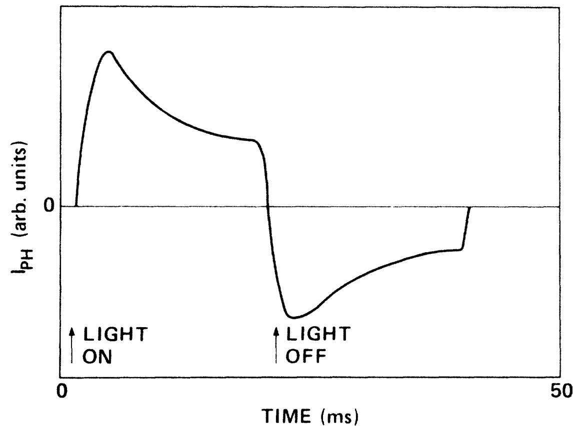

FIG. 8. Photocurrent versus time for 0.9-eV light. The photocurrent actually decreases as the illumination time increases and an equal but opposite polarity current appears upon termination of the illumination.

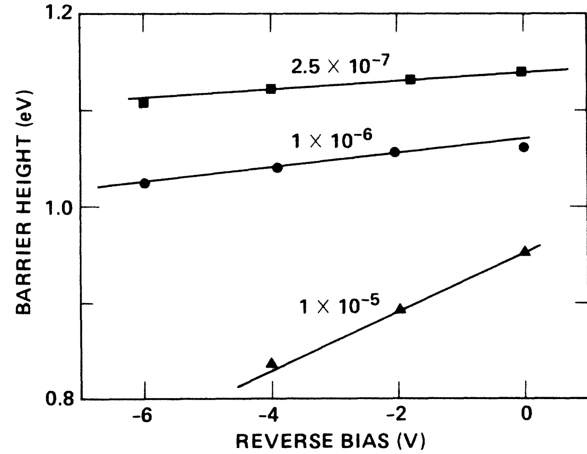

FIG. 9. The points indicate measured barrier height versus reverse bias for various doping levels. The solid lines indicate the barrier-height variation predicted using Eq. (8). Note that the dependence of the barrier increases as the doping increases.

the light is still present. When the illumination ceases, the electrons diffuse back to the positively charged defects, neutralizing the the space charge. The current flows in a negative direction; hence, during one cycle, no net charge flows in the external circuit. This conclusively demonstrates that the charge collection is determined by the carrier with the lowest mobility-lifetime product under conditions when the field distribution is affected by the photogenerated carriers. The collection length of the primary photocurrent is no longer the sum of the collection lengths of each individual carrier, as is the case when the carriers have sufficient mobility to avoid space-charge buildup.[22] The smaller fringes of this component are a further indication that this mechanism is correct. Transition C occurs throughout the sample, unlike the internal photoemission, transition A, and therefore exhibits smaller interference fringes due to spatial averaging.

The dependence of the effective barrier height on the field was also determined from the photoresponse measurements. The barrier heights as a function of reverse bias for various doping levels are shown in Fig. 9. For the lowest doping levels, the barrier height decreases very slightly with larger negative bias while barriers on the more highly doped material exhibit considerable lowering as function of bias. Results could not be obtained for the highest doping levels since the reverse-bias current became too large to detect the internal photoemission contribution. Thus both the increased doping levels and the larger negative bias causes a disappearance of the barrier.

V. DISCUSSION

A. Comparison to tunneling model

The experimental results presented in the preceding section are analyzed in terms of the theory of thermionic-field-emission theory discussed in Sec. II. The major points of comparison are the dependence of the effective barrier height on doping and field, the voltage dependence of the reverse-bias current, and the doping and temperature dependence of the ideality factor.

Consider first the dependence of the effective barrier on doping. The thermionic-field-emission theory predicts that the effective barrier height for 0-V reverse bias is given by $\varphi_{\text{eff}}=kT\varphi_b/qE_0$. Since E_0 gets larger with doping, the effective barrier height decreases. The reduction in the effective barrier can be calculated assuming that N_d is given as in Table I and $\epsilon_s m_r=0.5$ and using Eqs. (3), (5), and (8) for $V_r=0$ and $\varphi_b=1.14$ eV. The calculated effective barrier as a function of doping is depicted in Fig. 7 by the solid line, and is compared to the experimental barrier height corrected to 0-V applied bias. The reduction of the barrier height due to doping is reasonably well predicted by the theory, and can thus be ascribed to tunneling. Both theory and experiment indicate that the barrier height begins to exhibit a strong dependence on doping for levels above 10^{-5}. At this threshold doping level, the defect density is sufficiently high to cause significant reduction of the effective barrier even at zero field. The dominant current path is no longer over the top of the barrier but moves to lower energy. For a phosphorus doping of 10^{-3} when $E_{00}\sim kT$, the current tunnels predominately through the barrier at roughly half the height of the barrier. The critical doping level for barrier height variation predicted by theory is slightly higher than that observed suggesting that the actual tunneling is somewhat underestimated by the theory. This difference is quite likely due to either the assumption of parabolic bands in the calculation, difficulty in determining the exact doping density, and/or the effects of band-tail tunneling just below the mobility edge on the actual barrier height.

When the depletion region decreases, the tunneling current becomes very sensitive to the applied reverse bias. A small increase of the bias will decrease the effective barrier height significantly. The dependence of the effective barrier height on bias has been calculated for several doping levels and the results are compared to experiment in Fig. 9 and Table I. Two aspects should be noted. The calculated linear dependence of the barrier height on re-

verse bias agrees with experiment. The observed increase of the slope with increased doping is also in good agreement.

For diodes where tunneling is important, the reverse-bias current will not saturate at low voltages. If the experimentally observed changes of the barrier height with bias (Fig. 9) are inserted into Eq. (1), the solid curves in Fig. 4 result. The quantity J_{s0} was not computed from Eqs. (4) and (5) but rather adjusted to match each curve at zero bias. Good agreement for the various lower doping levels is observed; the slope of the reverse saturation current increases with doping exactly as predicted from the theory. At higher doping levels, the approximate tunneling theory of Sec. II slightly underestimates the change of the barrier height with voltage. From Eq. (9), we see that for the case of low doping levels the slope is proportional to the donor (or defect) density.

Finally, the tunneling contribution to the current also explains the increase dependence of the ideality with doping and with temperature. In Fig. 5, the calculated ideality factor from Ref. 5 is plotted as a function of the parameter kT/E_{00} along with the experimental ideality factor for a 10^{-5}-P-doped sample for different temperatures and for different dopings at room temperature. The trend is quite consistent indicating that both the doping and temperature dependence of the ideality factor are reasonably well predicted by the thermionic-field-emission theory. As in the case for the other barrier properties, Fig. 5 indicates that the theory somewhat underestimates the effect of tunneling.

In the above discussion, we have shown that there is rather good agreement between experiment and the approximate tunneling theory of Sec. II. It is also important to examine possible explanations for the small differences between theory and experiment.

The primary difference between theory and experiment is that the theory tends to underestimate the importance of tunneling. Changes of the barrier heights and ideality factors occur at slightly lower doping levels than predicted. This difference has several possible origins. First, the approximation of a Gaussian tunneling distribution tends to underestimate the tails of the distribution and, consequently, the tunneling contribution is underestimated.[5] A second more likely explanation is that the exact defect density is unknown. If the defect density is taken to depend on doping according to the relation $N_d \sim [PH_3]^{0.7}$, better agreement is obtained. Finally, one would expect that resonant tunneling of the electron from the metal through a localized band-tail state into the extended states of the semiconductor would become increasing important as the barrier becomes narrower.

B. Implications of the tunneling model

The results of the preceding subsection demonstrated that the tunneling model explains the observations rather well. We discuss next the implications of these results for the interpretation of various measurements. In particular, the effect of tunneling on flat-band measurements, the use of ideality measurements to determine interface quality, and the doping-induced lowering of the barriers are explored.

First, we consider the effects of tunneling on the use photocurrents to determine the built-in potential. The voltage dependence of the photocurrent is often used to determine the built-in potential of the barrier by noting the voltage at which the photocurrent changes sign. The tunneling through the barrier explains why the reversal of the sign of the photocurrent does not yield the correct built-in potential at high doping levels. For low doping, the photocurrent follows the relation[23]

$$I_{ph}(V)=I_0[1-\exp(l/l_c)] \\ =I_0\{1-\exp[B(V_b-V)^{1/2}]\}\ , \quad (14)$$

where l_c is the depletion width, I_0 is the photocurrent for very large reverse bias, B is a constant which depends on doping, etc., and V is the applied bias (positive for forward bias). If the quantity $\ln^2[1-I_{ph}(V)/I_0]$ is plotted versus the applied bias as in Fig. 10, the result should yield a straight line whose intercept is the built-in potential. For the lowest doping level this result yields 0.7 eV, which is not far from that derived from the barrier-height and activation-energy results. For higher doping levels, the form of Eq. (14) will be significantly modified since the barrier height becomes bias dependent. The result is curved plots rather than straight lines with intercepts which are incorrect. The built-in potential determined from the voltage dependence of the photocurrent (solid triangles) will be reduced compared with the expected built-in potential due to tunneling (open triangles), a result observed in this study (Fig. 11).

Second, the increase of the ideality factor due to tunneling complicates the separation of the recombination current from the thermionic-emission current used previously.[17] In general, the ideality factor for a recombination-dominated current is 2, while for the thermionic emission, it is nearly 1. While one would expect that increasing the number of defects in the material would increase the recombination, it also causes increased tunneling; in both cases the ideality factor increases. Consequently, one cannot rely on the ideality factor to

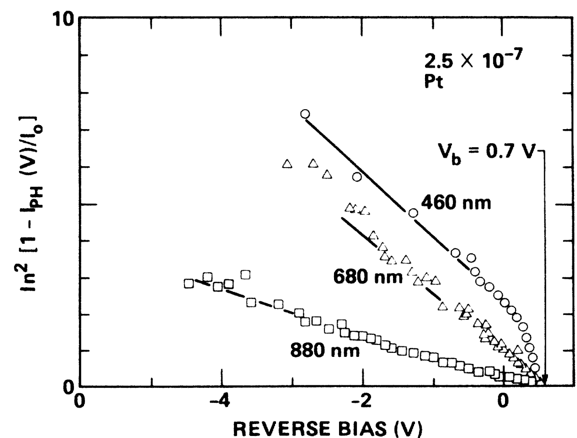

FIG. 10. Determination of the built-in potential using the variation of the photocurrent with applied bias. The built-in potential is estimated to be 0.7 V for the low doping.

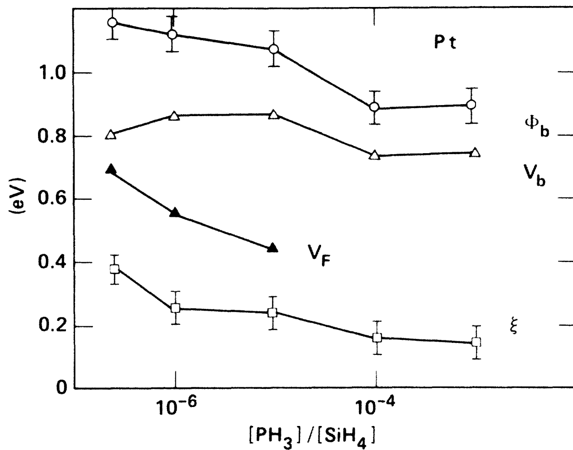

FIG. 11. Tunneling-corrected barrier height φ_b determined from Eq. (8) (circles), the activation energy ζ (squares), the built-in potential $V_b=\varphi_-\zeta$ (open triangles), and the flat-band voltage determined by the voltage dependence of the photocurrent (solid triangles) versus gas-phase doping concentration.

separate out the recombination current since tunneling through a defect-free interface will also yield ideality factors significantly larger than 1. The good general agreement between the thermionic-field emission suggests that the dominant source of large ideality factors is due to tunneling rather than recombination. It is unlikely that the recombination exhibits both the observed temperature and doping dependence depicted in Fig. 5.

The agreement between experiment and the thermionic-field-emission theory allows us to estimate the true barrier height and to correct for the effects of tunneling. Using Eq. (8) to solve for φ_b, the corrected barrier height is plotted versus doping in Fig. 11. There is an apparent small decrease ($\sim$0.25 eV) of the barrier for doping greater than 10^{-5}. However, one must include the fact that the approximate theory tends to underestimate the true tunneling, particularly for doping above 10^{-5} levels, by about 0.2 eV, the difference between the solid line and the triangles in Fig. 7. When this underestimation is added to φ_b in Table I, the actual tunneling-corrected barrier φ_b^* is found to be $\sim$1.1 eV independent of doping (Table I). Consequently, there is no evidence that the tunneling barrier lowers as a function of doping.

The above results have important consequences for the interpretation of previous results. The relatively abrupt onset of the effective barrier lowering as a function of doping and large barrier decrease (up to $\sim$0.6 eV) due to tunneling could easily be attributed to a specific doping level. The results in Fig. 7 and Table I demonstrate that reduction of the effective barrier due to tunneling without a specific level exhibits nearly exactly the same behavior at the observed densities. The abrupt change is a consequence of the exponential dependence of the tunneling on the barrier thickness; once the barrier becomes narrow, its effective height decreases rapidly. It is not necessary to impose new levels or changes in the intrinsic barrier properties to account for the observations. Previous measurements failed to include the effects of tunneling on the barrier heights.[6-8,10,14,17] This result also explains the discrepancy between the Schottky-barrier studies and the transport measurements which do not find evidence for such a level.[19] Therefore, the results can be explained without resorting to a phosphorus-induced level 0.3 eV below the mobility edge.

C. The Schottky barrier and the built-in potential

The tunneling-corrected barrier heights are important for examining the physics of Schottky-barrier formation on amorphous semiconductors. The tunneling effects occur regardless of the mechanisms of barrier formation and hence obscure the changes in the real barrier determined by interface reactions and charge transfer. Figure 12 presents a schematic of the evolution of the bands for a Pt/*a*-Si:H contact determined by incorporating results of this study. On undoped material, the barrier height is 1.1—1.15 eV, resulting in a built-in potential of 0.4—0.45 eV. Upon light doping the built-in potential increases abruptly to 0.8 eV. The barrier height, however, remains virtually unchanged. This behavior, uncommon for crystalline Si, is expected in the traditional models for Schottky-barrier formation. The basic difference is that the Fermi energy of *a*-Si:H can routinely be placed in the gap, while for crystalline Si the Fermi energy is typically at the conduction- or valence-band edges. Furthermore, the larger barrier in *a*-Si:H is due to a larger band gap.

D. The "Ohmic contact"

Finally, using the thermionic-field-emission theory, we can estimate the structure of "Ohmic contacts" or $n^+(10^{-2}$ P)-Pt on *a*-Si:H. Extrapolating the results of Fig. 7 suggests that the effective zero-bias "barrier" for a 10^{-2}-P-doped sample is roughly 0.4 eV. Using Eq. (3) to calculate E_{00} and using the results of Crowell and Rideout indicates that at room temperature the tunneling path occurs at 0.08 eV from the conduction band in the

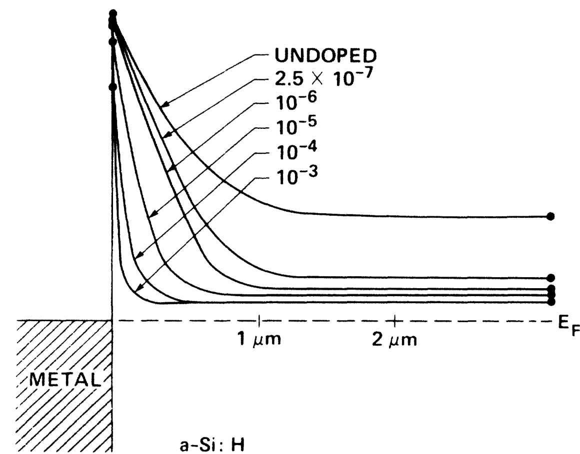

FIG. 12. Evolution of the Schottky barrier as the doping level increases for no applied bias. Note that the barriers become extremely narrow for the higher doping.

a-Si:H layer. Because the Fermi level in 10^{-2}-P-doped a-Si:H is $\sim$0.15 eV from the mobility edge, the total effective "barrier" the electrons must overcome for an n^+-Pt contact is roughly $\sim$0.23 eV. The barrier that the electrons must tunnel through is roughly 30 nm thick. If the metal is changed to Cr or Pd, the effective barrier becomes 0.06 eV, and the electrons must surmount a $\sim$0.21-eV barrier to enter the a-Si:H layer, a negligible difference. Hence, assuming an intimate contact at the metal—a-Si:H interface and that no unusual metal—a-Si:H interactions alter the defect density, changing of the metal should have a relatively small effect on the current injecting capability of an n^+ contact.

VI. CONCLUDING REMARKS

Well-characterized Schottky diodes on doped a —Si:H have been prepared with stable PtSi/a-Si:H interfaces. The electrical properties of the Schottky barrier have been measured and analyzed. It was found that significant effects on the effective barrier height and ideality factor due to tunneling were observed which are in good agreement with the approximate tunneling theory. Defining the true barrier height to be the energy difference between the metal Fermi energy and the conduction-band mobility edge of the a-Si:H at the interface, the results of this paper show that this barrier does not change with doping. Applied fields, lower temperatures, and doping cause increased tunneling and a lowering of the effective barrier to electron transport. The large change in the effective barrier for increased doping levels observed in previous work is due to tunneling from the metal through the barrier into the conduction-band extended states of the amorphous semiconductor.

The Schottky barrier on a-Si:H exhibits several similarities to barriers on crystalline Si. (1) The barrier height remains nearly constant independent of doping; (2) thermionic-emission and thermionic-field-emission transport are observed; (3) similar ideality factors ($\sim$1.05) are observed for doping levels up to 10^{-5}; and (4) there is little evidence of recombination at the interface. Significant differences are that (1) the barrier is $\sim$0.25 eV higher for a-Si:H diodes, and (2) the built-in potential changes significantly upon low doping levels. The large change in built-in potential is attributed to the change in bulk Fermi energy of the bulk a-Si:H and the other changes are attributed to band-gap differences. It has previously been shown that the Schottky barrier for different metals exhibits a constant difference for amorphous and crystalline Si. All of these results are consistent with the proposal that the effect that leads to the Schottky barrier are the same for both a-Si:H and single-crystal Si.

ACKNOWLEDGMENTS

We would like to thank R. Thompson for preparing the samples, and M. Stutzmann and R. Street for helpful discussions. This work was supported in part by a contract from the Solar Energy Research Institute (Golden, CO).

[1]For a review of the properties of Schottky barriers on hydrogenated amorphous silicon, see R. J. Nemanich in *Semiconductors and Semimetals,* edited by J. I. Pankove (Academic, New York, 1984), Vol. 21C, p. 375, or R. J. Nemanich and M. J. Thompson, *Metal-Semiconductor Schottky Barrier Junctions and Their Applications,* edited by L. Sharma (Plenum, New York, 1984).

[2]R. J. Nemanich, M. J. Thompson, W. B. Jackson, C. C. Tsai, and B. L. Stafford, J. Non-Cryst. Solids **59& 60**, 513 (1983).

[3]E. H. Rhoderick, *Metal-Semiconductor Contacts* (Clarendon, Oxford, 1978).

[4]F. A. Padovani and R. Stratton, Solid-State Electron. **9**, 695 (1966).

[5]C. R. Crowell and V. L. Rideout, Solid-State Electron. **12**, 89 (1969).

[6]P. Viktorovitch, G. Moddel, and W. Paul, in *Tetrahedrally Bonded Amorphous Semiconductors,* edited by R. A. Street, D. K. Biegelsen, and J. C. Knights (AIP, New York, 1981), p. 1.

[7]M. J. Thompson, N. M. Johnson, R. J. Nemanich, and C. C. Tsai, Appl. Phys. Lett. **39**, 274 (1981).

[8]C. R. Wronski and D. E. Carlson, Solid State Commun. **23**, 421 (1977).

[9]A. J. Snell, K. D. Mackenzie, P. G. LeComber, and W. E. Spear, Philos. Mag. B **40**, 1 (1979).

[10]J. Beichler, W. Fuhs, H. Mell, and H. M. Welsch, J. Non-Cryst. Solids **35& 36**, 587 (1980).

[11]C. R. Wronski, D. E. Carlson, and R. E. Daniel, Appl. Phys. Lett. **29**, 602 (1976).

[12]C. R. Wronski, B. Abeles, G. D. Cody, and T. Tiedje, Appl. Phys. Lett. **37**, 96 (1980).

[13]R. J. Nemanich, M. J. Thompson, W. B. Jackson, C. C. Tsai, and B. L. Stafford, J. Vac. Sci. Technol. B **1**, 519 (1983).

[14]T. Yamamoto, Y. Mishima, M. Hirose, and Y. Osaka, Jpn. J. Appl. Phys. **20**, Supp. 20-2, 185 (1981).

[15]R. A. Street, Phys. Rev. B **27**, 4924 (1983).

[16]R. J. Nemanich, M. J. Thompson, W. B. Jackson, C. C. Tsai, and B. L. Stafford, J. Non-Cryst. Solids **59& 60**, 513 (1983).

[17]A. Madan, W. Czubatyj, J. Yang, M. S. Shur, and M. P. Shaw, Appl. Phys. lett. **40**, 234 (1982).

[18]M. Stutzmann and R. A. Street, Phys. Rev. Lett. **54**, 1836 (1985).

[19]R. A. Street, J. Zesch, and M. J. Thompson, Appl. Phys. Lett. **43**, 672 (1983).

[20]R. Street, Phys. Rev. Lett. **49**, 1187 (1982).

[21]W. B. Jackson and N. M. Amer, Phys. Rev. B **25**, 5559 (1982).

[22]R. S. Crandall, RCA Rev. **42**, 441 (1981).

[23]R. S. Crandall, R. Williams, and B. E. Tompkins, J. Appl. Phys. **50**, 5506 (1979).